

EFFECT OF ASSEMBLY TYPES ON BOLTED CONNECTION STRENGTH CONSIST OF BUILT-UP ANGLE MEMBERS UNDER MONOTONIC TENSILE FORCE

Hideo HAIKATA¹, Kikuo IKARASHI², and Kazuya MITSUI³

SUMMARY

Steel angle is often utilized for braces in steel frame buildings, and when the braces are connected eccentrically in the out-of-plane direction of the gusset plate, bending moment due to the eccentricity acts about both principal axes of the braces. Therefore, the effective cross area in the current design procedure is derived by assuming that a part of the angle steel outstanding leg is ineffective. On the other hand, in the authors' earlier research, it is clarified that the connection strength is determined by the eccentric distance of the member centroid and the connection length, and highly accurate evaluation formulae for yield and ultimate resistance applicable from thin to thick plates are proposed for a single member. This study aims to clarify the effect of assembly types on the bolted connection strength consisting of built-up angle members subjected to tensile force and to examine whether the evaluation formulae for yield and ultimate resistance proposed in the earlier research apply to the built-up angle members.

Keywords: *steel angle member; eccentricity; effective area; bolt; connection; built-up member.*

INTRODUCTION

Low-rise steel-framed buildings such as warehouses and factories, which constitute large spaces, are expected to function as disaster prevention centers in a severe earthquake due to their high capacity and must ensure high earthquake resistance. Low-rise warehouses and factories are often constructed using lightweight steel construction, in which the structural members are generally composed of columns, beams, and braces. In this building type, braces resist a portion of the horizontal load acting on the structure, thereby reducing the deformation of the structure. Therefore, for a building to be resistant to horizontal loads such as earthquakes and strong winds, the bolted connection strength must be less than the allowable stress even when horizontal forces act on the structure. In other words, the ultimate strength of the brace connections must be sufficiently greater than the brace's axial yield strength to ensure the structure's seismic performance.

Although braces are often made of a single member with a steel angle, eccentric tensile forces are generated at the connections, resulting in highly non-uniform stresses in this case. The current design provision in Japan calculates the ineffective area using the ineffective length of the outstanding leg, which is determined according to the number of bolts shown in Table 1, and indirectly considers the effect of eccentric tensile forces (Architectural Institute of Japan, 2021). On the other hand, Nagasato et al.(2021) clarified that the bolted connection strength can be evaluated based on the eccentricity of the member and the total distance between bolt holes, and proposed highly accurate strength formulae for a single member that can be applied to both thin and thick plates. However, it is necessary to understand the effect of assembly, since steel angles are often used as the built-up members. In this study, tensile tests of bolted connections are conducted on a single member and the built-up members with steel angles to clarify the effect of assembly types on the bolted connection strength consisting of the built-up angle

¹ Graduate Student, Dept. of Arch. and Build. Eng., Tokyo Institute of Technology, Japan, e-mail: haikata.h.aa@m.titech.ac.jp

² Professor, Dept. of Arch. and Build. Eng., Tokyo Institute of Technology, Japan, e-mail: ikarashi.k.aa@m.titech.ac.jp

³ Assistant Professor, Dept. of Arch. and Build. Eng., Tokyo Institute of Technology, Japan, e-mail: mitsui.k.ad@m.titech.ac.jp

members subjected to tensile force, and to examine whether the evaluation formulae for yield and ultimate strength proposed in Nagasato et al.(2021) apply to the built-up angle members as well.

Table 1: *Ineffective length of outstanding leg at ultimate strength (Architectural Institute of Japan, 2021) h_n*

Number of bolts n	1	2	3	4	5
Ineffective length of outstanding leg h_n	$h - t$	$0.7 h$	$0.5 h$	$0.33 h$	$0.25 h$

TENSILE TESTS OF BOLTED CONNECTIONS OF BUILT-UP ANGLE MEMBERS

Overview of the Experiment

In this study, monotonic tensile tests are conducted to investigate the bolted connection strength of the single member and the built-up members with steel angles. As shown in Figure 1, the angle members are used as the braces, and the connection leg length b and the outstanding leg length h are 50 mm, the thickness of angle t is 2.3 mm, and the bolt hole diameter d is 17 mm, which are the same for all specimens. The number of bolts at the bolted connections n is set to 3, the bolt spacing p is set to 40 mm, the edge distance parallel to the direction of stress e_1 is set to 40 mm, and the distance from the hole center to the edge toward which the force is directed e_2 is set to 25 mm, which are also the same for all specimens. As shown in Figure 2, to investigate the effect of the distance l between the first bolt holes, only specimen A6 is set to $l = 1000$ mm, and all the remaining specimens are set to $l = 1200$ mm. The experimental variables are the cross-sectional geometry of the specimens and the bolt geometry.

The cross-sectional shapes are classified into a single member, member(Series A), which consists of connection legs built-up back-to-back across the gusset plate, and member (Series B), which consists of outstanding legs built-up back-to-back, as shown in Figure 1. To investigate the effect of spacing between the joint bolts, the spacing of A3 and A4 in Series A is set to 600 mm and 1000 mm, respectively, while the spacing of B2 and B3 in Series B is varied to 1000 mm and 600 mm, respectively. The joint bolts are placed in the middle of the length of the brace in A2, A2Re, B4, B6, B7, and B9 to examine the effect of the presence or absence of bolts placed in the middle of the length of the brace. Specimens B1, B5, and B7 in Series B are also jointed at 60 mm from the end of the member to restrain the deformation of the outstanding leg that occurs at the end of the member due to tensile force. Specimens A5 and B8 have five and nine joint bolts, respectively, to investigate the effect of increasing the number of joint points. The high-strength bolts M16 used and pre-tension is not installed.

The displacement transducers are installed as shown in Figure 3, and the elongation between the first bolt holes is measured, with the average value used as the displacement δ . A monotonic unidirectional load is applied to the braces at both ends using an Amsler-type testing machine. Table 2 shows the definitions of the symbols used in this study. Table 3 shows the material properties obtained from coupon tests.

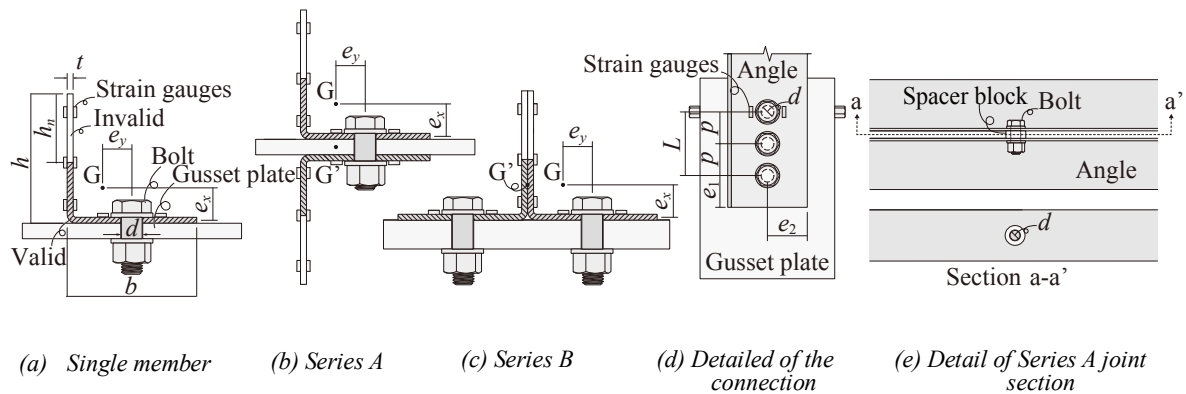


Figure 1: *Dimensions of the specimen and detail of the connection*

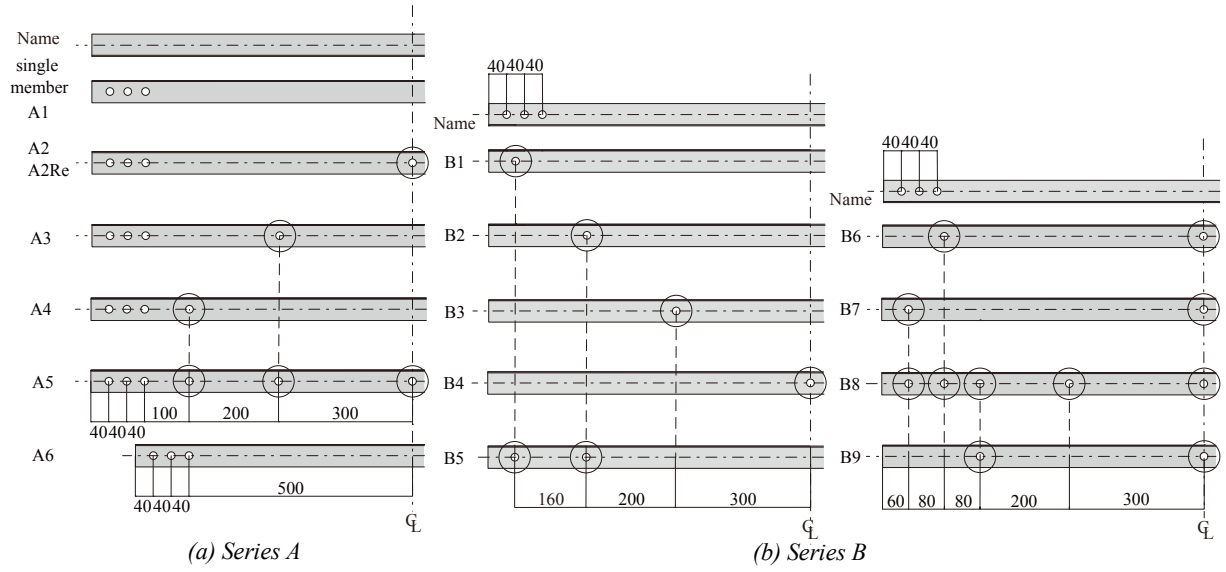


Figure 2: Configuration of specimens

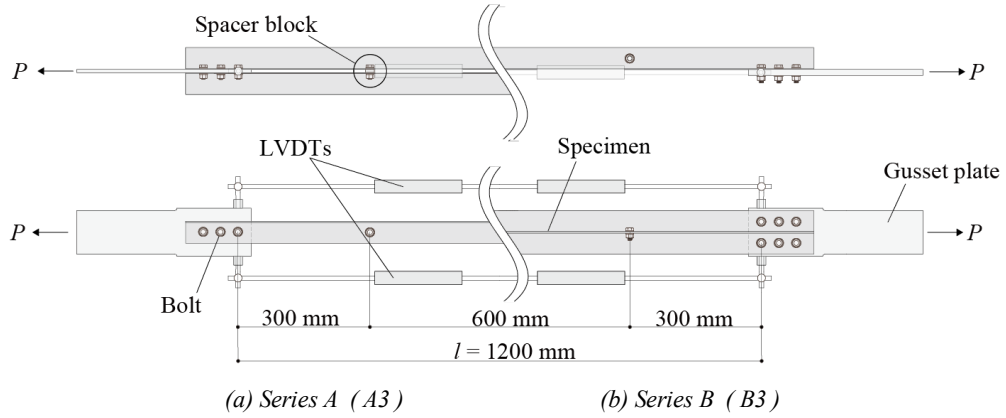


Figure 3: Shape of specimen (A3, B3)

Table 2: Definition of symbols

A_n : Net area	σ_y : Yield stress of brace
b : Connection leg length (50 mm)	σ_u : Tensile strength of brace
h : Outstanding leg length (50 mm)	eP_y : Yield strength obtained from experimental test
d : Bolt hole diameter (17 mm)	eP_u : Ultimate strength obtained from experimental test
p : Bolt spacing (40 mm)	P_u : Calculated ultimate strength (without considering ineffective length of outstanding leg)
t : Thickness of angle (2.3 mm)	cP_y : Calculated yield strength (without considering ineffective length of outstanding leg)
e_1 : Edge distance parallel to the direction of stress (40 mm)	cP_u : Calculated ultimate strength (without considering ineffective length of outstanding leg)
e_2 : Distance from the hole center to the edge toward which the force is directed (25 mm)	β : rate of reduction
$L(=p(n-1))$: Total distance between bolt holes	U_y : Reduction factor for yield strength
J_y : Joint efficiency at yield strength	U' : Reduction factor for ultimate strength
J_m : Joint efficiency at ultimate strength	S_y : Calculated yield strength according to Nagasato et al. (2021)
	S_u : Calculated ultimate strength according to Nagasato et al. (2021)

Table 3: Mechanical properties of steel

Thickness t [mm]	Yield stress σ_y [N/mm ²]	Tensile stress σ_u [N/mm ²]	Young's modulus E [N/mm ²]	Yield ratio $Y.R.$ [%]	Elongation ϵ_u [%]
2.3	274	441	192000	61.8	26.8

Effect of Assembly Types on Bolted Connection Strength Consist of Built-up Angle Members

Figure 4 shows the definition of yield strength eP_y , and Table 4 shows the calculated yield strength cP_y based on Eq. (1) and the calculated ultimate strength cP_u based on Eq. (2), which are given in Architectural Institute of Japan(2021), respectively. The cross-sectional area A_n excluding bolt holes is used.

$$cP_y = (A_n - ht/2) \sigma_y \quad (1)$$

$$cP_u = (A_n - hnt) \sigma_u \quad (2)$$

$$A_n = bh - (b - t)(h - t) - dt \quad (3)$$

Table 4 summarizes the experimental results. In all specimens, the cracks initiate from the side of the first bolt hole as shown in Figure 5, and the resistance decreased with crack propagation, resulting in effective cross-sectional rupture. Deformation of the outstanding legs is also observed in the single member and the specimens without member end ties.

Figure 6 shows the load-displacement relationship. In the figure, ∇ stands for the yield strength eP_y defined by the method shown in Figure 4, and \blacktriangledown stands for the ultimate strength eP_u . The vertical axis is normalized by the ultimate strength based on the effective cross-sectional area, and the horizontal axis is displacement δ normalized by displacement δ_u at ultimate strength. The following equation, J_m , which is the value of the ultimate strength divided by P_u , is used in the following discussion.

$$P_u = A_n \sigma_u \quad (4)$$

$$J_m = eP_u / P_u \quad (5)$$

Figure 6(a) shows the experimental results for the same model, A2, and A2Re. Since there is some scatter even for the same model under the same conditions, this degree of scattering is unavoidable by the experimental investigation. Figure 6(a) shows the effect of spacing between joint bolts in Series A, and Figure 6(b) shows the effect of bolts placed in the center and at the ends of the member in Series B. There is a slight difference in J_m in both Figures 6(a) and 6(b), and the effect of the difference in joint bolt position on the ultimate strength is small. In other words, there is no effect on the increase in resistance when the joint bolt position is varied within the range of this study, or when the joint bolts are used to restrain the out-of-plane deformation that occurs at the ends of the outstanding legs, as shown in Figure 5.

In addition, Figure 6(c) shows the effect of assembly for a single member and Series A, and Figure 6(d) shows the effect of different assembly types for Series A and Series B. The J_m values are slightly higher for the single member in Figure 6(c) and for Series A in Figure 6(d); however, there is no significant difference in either case. Since the ultimate strength per angle member is almost the same for the single member and the built-up members of the same cross-section, and the ultimate strength of single members is affected by the eccentricity from Nagasato et al.(2021), it is appropriate to consider the eccentricity when regarded as a single independent member, rather than the eccentricity when regarded as a unit member after assembly for the ultimate strength in the built-up members.

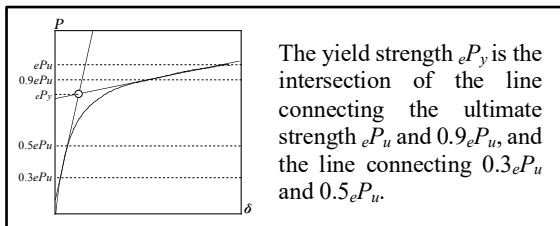


Figure 4: Definition of yield strength

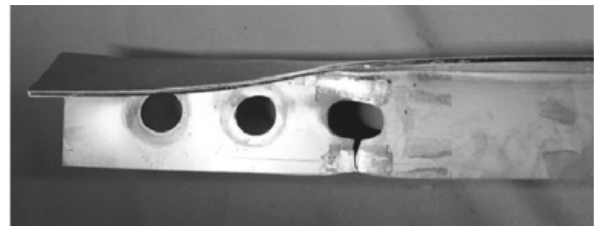


Figure 5: Effective cross-sectional rupture

Table 4: Calculation and experimental results

Specimen	Calculated strength[kN]		Test results[kN]	
	eP_y	eP_u	eP_y	eP_u
Single member	35.1	56.5	49.1	59.0
A1	70.2	113	92.6	112
A2			91.1	109
A2Re			93.5	114
A3			96.8	113
A4			94.3	113
A5			98.5	115
A6			96.2	116
B1			94.2	115
B2			91.9	113
B3			92.5	110
B4			89.4	110
B5			92.3	110
B6			86.2	107
B7			94.6	114
B8			94.6	113
B9			96.4	113

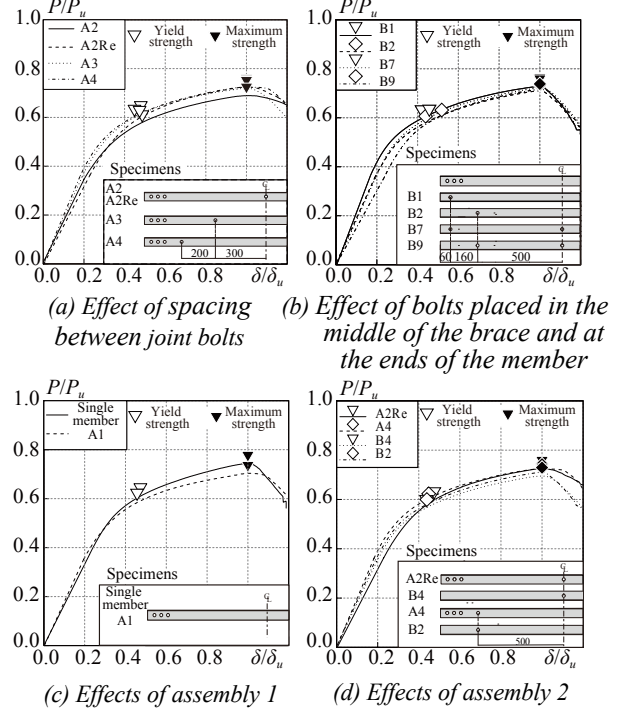
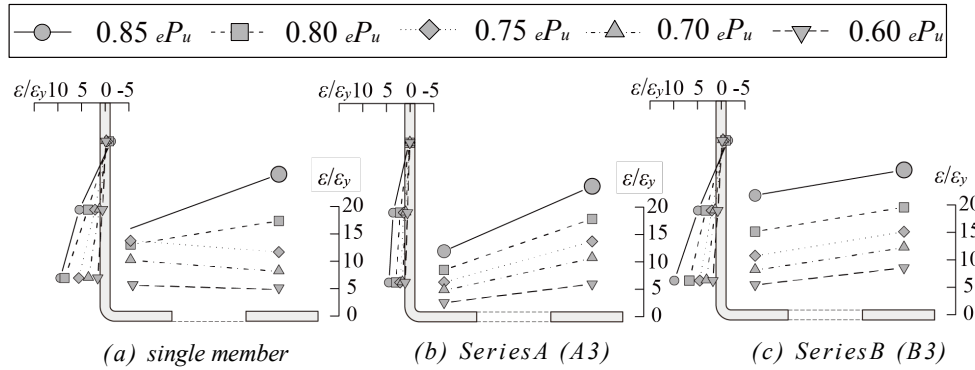
**Figure 6: Load-displacement relationship**

Figure 7 shows the strain distribution as the load increases. The strain ε shown in each axis is normalized by the strain ε_y at the yield stress, with positive values representing the strain under tensile stress. The strain distribution at the outstanding leg of Series A (Figure 7(b)) is less biased than that of the single member and Series B. Therefore, it can be said that the out-of-plane eccentricity is smaller. The strain distribution at the connection leg of Series B (Figure 7(c)) shows less biased than that of the single member and Series A. Therefore, it can be said that the in-plane eccentricity is smaller. On the other hand, the strain distribution when $0.85eP_u$, before the ultimate strength, is applied (shown in \bullet) shows that the strain near the bolt holes on the free end side of the connection legs, which is the rupture position, is of the same magnitude regardless of the assembly type. The strain at the free end of the connection leg under this load is much higher than the yield strain of the steel.

Although the out-of-plane eccentricity and in-plane eccentricity can be reduced by differences in the assembly types, the ultimate strength is considered to be affected by the eccentricity when the assembled cross-section at the first bolt-hole position is regarded as independent single members, not when it is regarded as a unit member. This causes a stress concentration at the free end of the connection leg, and when the strain reaches a certain value, a crack is generated and the ultimate strength is reached. Therefore, the effect of differences in the position of joint bolts and assembly types on the ultimate strength is considered to be small.

**Figure 7: Strain distribution change at the first bolt hole location**

VALIDITY OF FORMULAE FOR CALCULATING YIELD AND ULTIMATE STRENGTH OF BUILT-UP ANGLE MEMBERS

Current Design Formula for Bolted Connection

Figure 8 shows the correspondence between the yield strength eP_y obtained from the experimental tests and the calculated cP_y . The yield strength cP_y is derived from Eq. (1) given in Architectural Institute of Japan(2021). The connection strength of the double-use (Series A) specimen in Tatsumi et al.(2017) is also plotted. With the exception of a few specimens, most of the specimens are evaluated on the safe side according to the current design formula; however, the formula underestimates by up to 40 % compared to the experimental tests of the specimens in this study and underestimates by up to 60 % compared to the experimental results of the specimens in Tatsumi et al.(2017).

Figure 9 shows the relationship between the ultimate strength eP_u obtained from the experimental tests and the calculated result cP_u . The result cP_u is calculated using Eq. (2), which is given in Architectural Institute of Japan(2021). The connection strength of the double-use (Series A) in Tatsumi et al.(2017) and Fujimoto et al.(1993) is also plotted. For many of the specimens in Fujimoto et al.(1993), the calculated results are not evaluated on the safe side. The difference between the experimental and calculated results is within $\pm 30\%$.

Based on the above, it is confirmed that the current design formula for the bolted connection, which uses the ineffective length of the outstanding leg determined according to the number of bolts in the Architectural Institute of Japan(2021), underestimates or overestimates the strength of some experimental results.

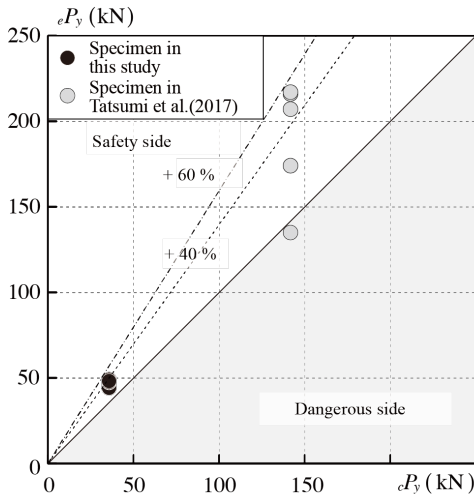


Figure 8: Comparison of experimental results and yield strength calculation based on the guideline

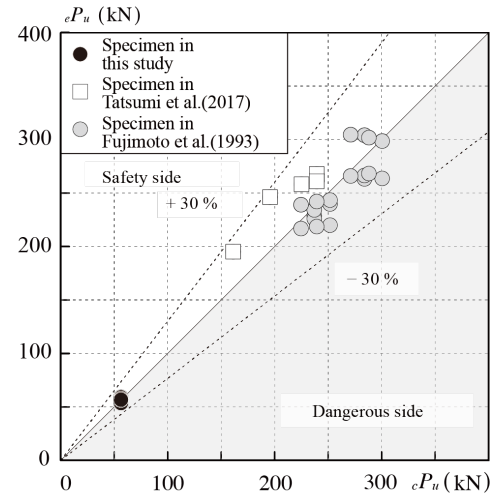


Figure 9 : Comparison of experimental results and ultimate strength calculation based on the guideline

Evaluation Formula for Yield Strength of Built-up Member Subject to Tensile Force

The method of applying the evaluation formula for the yield strength of a single member, which considers the eccentricity and the total distance between bolt holes L that affect the resistance proposed in Nagasato et al.(2021), to the built-up members is discussed. The reduction factor U_y shown in Table 2 is obtained by Eq. (6) proposed in Nagasato et al.(2021).

$$U_y = 1 - 0.75 \sqrt{e_x^2 + e_y^2} / L \geq 0.4 \quad (6)$$

The reduction factor U_y considers the influence of the eccentricity e_x and e_y and the total distance between bolt holes L as shown in Figure 1. The eccentricity is determined by the centroid's position and the bolt holes' position in the cross-section. The centroid of the cross-section is point G in Figure 1 when the member is regarded as an independent single member, and the centroid is point G' in Figure 1 when the member is assumed to behave as a unit member. In this case, the out-of-plane eccentricity e_x for Series A and the in-plane eccentricity e_y for Series B is zero.

Figures 10(a) and 10(b) show the relationship among $\sqrt{e_x^2 + e_y^2}/L$, the joint efficiency J_y , which is the yield strength divided by yield stress σ_y and the net area A_n , and the reduction factor U_y , as calculated by Eq. (7) for the specimens when regarded as an addition of an independent single member and when regarded as a unit member, respectively.

$$J_y = eP_y / A_n \sigma_y \quad (7)$$

The experimental results for a single member in this study and by Nagasato et al.(2021) are shown in Figure 10. Table 5 shows calculated values of the eccentricity rate, J_y and U_y . Comparing these results, Figure 10(b) shows a better correspondence with U_y ; however, the variation of the built-up members in Figure 10(a) is comparable to that of the single member, which can be evaluated when regarding the built-up members as an addition of independent single members. Therefore, considering the correspondence with the ultimate strength evaluation discussed later, the yield strength per angle member S_y , shown in Table 2, is calculated using the eccentricity when the built-up member is regarded as an addition of independent single members. The calculated yield strength S_y can be obtained by the following equation.

$$S_y = U_y A_n \sigma_y \quad (8)$$

Figure 11 shows the relationship between the yield strength eP_y obtained from the experimental results and the calculated S_y . The horizontal axis represents the calculated results and the vertical axis represents the experimental results. The yield strength S_y is calculated by Eq. (8) proposed by Nagasato et al.(2021). The connection strength of the double-use (Series A) specimen in Tatsumi et al.(2017) is also shown. It can be confirmed that all specimens in this study are evaluated on the safe side. The difference between the experimental and calculated results is within $\pm 25\%$, indicating a good correspondence. On the other hand, some experimental results conducted by Tatsumi et al.(2017) are not evaluated on the safe side. This is because the reduction factor U_y obtained by Eq. (9) is determined so that it can be evaluated on the safe side concerning the yield strength obtained by the method shown in Figure 4, while in Tatsumi et al.(2017), the yield strength is defined as “the strength at the point when the tangential stiffness decreases to about 1/20 to 1/10 of the initial stiffness.” The difference in the method used to determine the yield strength is considered to have resulted in the evaluation on the dangerous side. Therefore, the experimental results can be evaluated on the safe side by determining the yield strength using the method of this paper and by Nagasato et al.(2021).

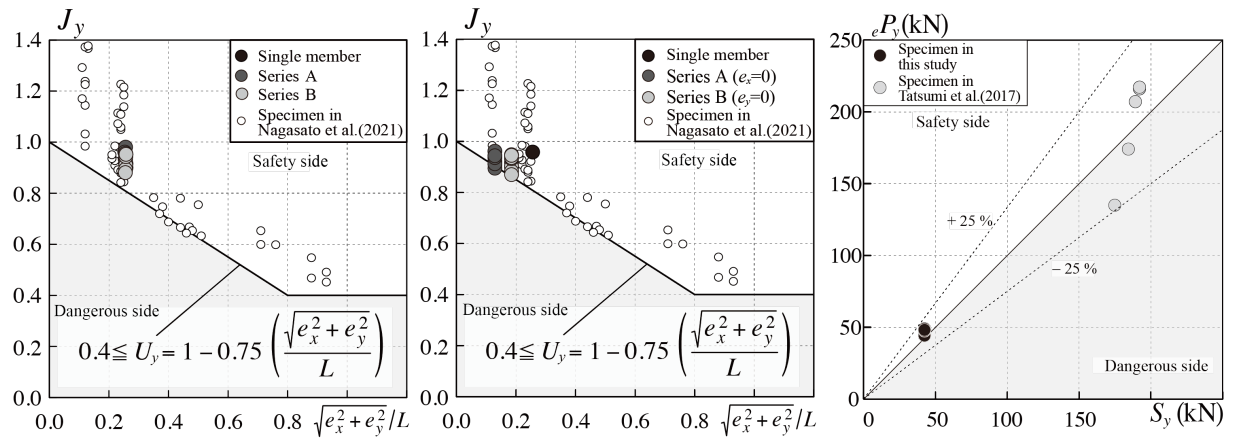


Figure 11: Validation of yield strength calculation formula

Figure 10: Relationship between joint efficiency J_y and eccentricity $\sqrt{e_x^2 + e_y^2}/L$

Table 5: Relationship between joint efficiency J_y and reduction factor U_y

Name	$\sqrt{e_x^2 + e_y^2}/L$		J_y	U_y	
	(a)	(b)		(a)	(b)
Single member	0.225	0.225	0.951	0.831	0.831
A1		0.129	0.910		0.903
A2			0.895		
A2Re			0.921		
A3			0.912		
A4			0.961		
A5			0.936		
A6			0.944		
B1		0.185	0.948		0.861
B2			0.898		
B3			0.917		
B4			0.902		
B5			0.883		
B6			0.870		
B7			0.932		
B8			0.937		
B9			0.946		

Evaluation Formula for Ultimate Strength of Built-up Member Subject to Tensile Force

The ultimate strength evaluation formula for a single member that considers eccentricity and the total distance between bolt holes is proposed by Nagasato et al.(2021) and applied to the built-up members. The reduction factor U' shown in Table 2 is obtained by Eq. (9) according to Nagasato et al.(2021).

$$U' = 1 - 1.2 \sqrt{e_x^2 + e_y^2}/L \geq 0.4 \quad (9)$$

Figure 12 shows the relationship among $\sqrt{e_x^2 + e_y^2}/L$, the joint efficiency J_m and the reduction factor U' for each specimen (a) when regarded as an addition of independent single members and (b) when regarded as a unit member. The experimental results of this study and those of previous studies on single members (Nagasato et al. 2021, Tatsumi et al. 2017, Tanaka et al. 1983, Yip et al. 2000, LaBouble et al. 1995, Paula et al. 2008) are also shown in the figure. Table 6 shows calculated values of the eccentricity rate, J_m and U' . Based on the evaluation formula proposed by Nagasato et al.(2021), it can be seen from Figure 12(a) that the proposed formula shows a good correspondence with the evaluation formula when the built-up member is evaluated as an addition of independent members. On the other hand, when the built-up member is considered as a unit member, and the out-of-plane eccentricity e_x is set to 0 for Series A, and the in-plane eccentricity e_y is set to 0 for Series B, the evaluation is slightly on the dangerous side, as shown in Figure 12(b). Therefore, the ultimate strength per angle member S_u' , shown in Table 2, is calculated using the eccentricity when the built-up member is regarded as an addition of independent single members. The calculated ultimate strength S_u' is calculated by Eq. (11) using the reduction factor β obtained by Eq. (10). The reduction ratio β is determined by the bolt hole-to-diameter ratio d/b , which is a shape factor affecting the joint efficiency J_m . All specimens in this study have $\beta = 1.0$.

$$\beta = 0.6 + 1.2 d / b \leq 1.0 \quad (10)$$

$$S_u' = \beta U' P_u \quad (11)$$

Figure 13 shows the relationship between the ultimate strength eP_u obtained from the experimental results and the calculation results S_u' . The horizontal axis represents the calculated results and the vertical axis represents the experimental results. The ultimate strength S_u' is derived from Eq. (11) proposed by Nagasato et al.(2021). The connection strength of the double-use (Series A) specimens in Tatsumi et al.(2017) and Fujimoto et al.(1993) are also shown. Although some specimens are evaluated on the dangerous side, the difference between the experimental and calculated results is within $\pm 30\%$, indicating a good correspondence.

These results indicate that the resistance of bolted connections of the built-up members subjected to tensile forces can be accurately calculated by using the eccentricity when the built-up member is regarded as an addition of

independent single members. This can be related to the fact that, as shown in Figure 7, the strain at the free end of the connection leg where the crack occurs is of similar magnitude regardless of the assembly type at the point where $0.85eP_u$ acts before the ultimate stress. In other words, the resistance of the built-up members is determined by the increase in the strain at the free end of the crack connection leg up to a certain magnitude, and the value of the strain at this point is considered to be affected by the eccentricity of the single member that constitutes the assembly.

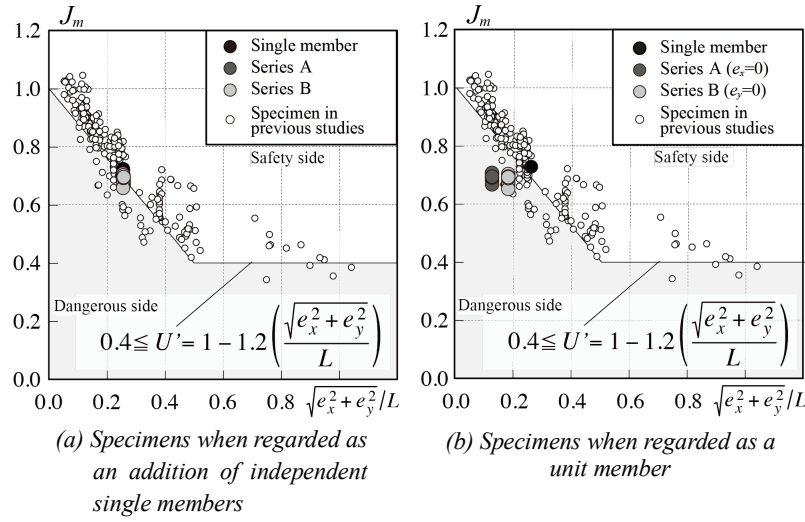


Figure 12: Relationship between joint efficiency J_m and eccentricity $\sqrt{e_x^2 + e_y^2}/L$

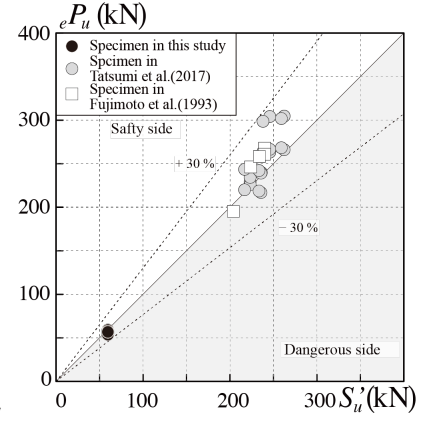


Figure 13: Validation of the ultimate strength calculation formula

Table 6: Relationship between joint efficiency J_m and reduction factor U'

Name	$\sqrt{e_x^2 + e_y^2}/L$		J_m	U'	
	(a)	(b)		(a)	(b)
Single member		0.225	0.703		0.730
A1			0.687		
A2			0.672		
A2Re			0.671		
A3		0.129	0.674		0.846
A4			0.652		
A5			0.694		
A6			0.689		
B1			0.703		0.730
B2			0.687		
B3			0.672		
B4			0.671		
B5		0.185	0.674		0.778
B6			0.652		
B7			0.694		
B8			0.689		
B9			0.692		

CONCLUSIONS

In this study, tensile tests on the bolted connection of the built-up angle members are conducted to clarify the effects of assembly types on bolted connection strength and to examine whether the evaluation formulae for yield and ultimate resistance proposed by Nagasato et al.(2021) apply to the built-up angle members. The following is a summary of the findings of this study.

Experiments conducted by varying the assembly type and position of joint bolts revealed that the effect of assembly types and position of joint bolts on the ultimate strength is small. This is because the resistance of the built-up members contributes to the eccentricity when regarded as a single independent member, and varying joint bolts do

not provide sufficient restraint to increase the resistance.

Yield strength of the built-up members can be calculated more accurately than the current yield strength calculation formula using the eccentricity when the built-up member is regarded as an addition of independent single members. However, some specimens is not evaluated on the safe side due to differences in the method of determining the yield strength.

Ultimate strength of the built-up members can be calculated more accurately than the current ultimate strength formula by using the eccentricity when the built-up member is regarded as an addition of independent single members.

The resistance of the built-up angle members is determined by the increase in the strain at the free end of the connection leg where rupture occurs, and the strain is considered to be affected by the eccentricity of the single member that built-up the assembly.

REFERENCES

Architectural Institute of Japan, *Recommendation for the Design of Connection in Steel Structures*, 2021.2

A. S. Yip, J. J. R. Cheng, "Shear Lag in Bolted Cold-Formed Steel Angles and Channels in Tension", Structural Engineering Report 133, University of Alberta, 2000. 9, <https://doi.org/10.7939/R3J09WD3T>

A. Tanaka, H. Naruhara and H. Aoki, "Experimental Study on the Connections of Steel Channel Braces", Summaries of Technical Papers of Annual Meeting, Architectural Institute of Japan, pp.1319 - 1320, 1983. 7

Kazuma NAGASATO, Kikuo IKARASHI, Kazuya MITSUI, "Strength of Bolted Steel Structural Members under Eccentric Tension", Journal of Structural and Construction Engineering (Transaction of AIJ), Vol.86, No.789, pp.1570-1580, 2021.11, <https://doi.org/10.3130/aijs.86.1570>

M. Fujimoto, T. Namba, T. Nakagome, T. Nishiyama, H. Shimokawa, and K. Kubota, "Experimental Study on Seismic Safety of The Steel Brace Joints", Journal of Structural and Construction Engineering (Transaction of AIJ), No.445, pp.127 - 137, 1993. 3, https://doi.org/10.3130/aijsx.445.0_127

N. Tatsumi, S. Kishiki, "Effects of Connection Detail on Strength And Cyclic Deformation Capacity of Angle Brace", Journal of Structural and Construction Engineering (Transaction of AIJ), Vol. 82, No. 736, pp. 909-919, 2017.6, <https://doi.org/10.3130/aijs.82.909>

R. A. LaBouble, W. W. Yu, "Tensile and Bearing Capacities of Bolted Connections, Final Summary Report", Civil Engineering Study 95-6, University of Missouri - Rolla, 1995

V. F. Paula, L. M. Bezerra, W. T. Matias, "Efficiency reduction due to shear lag on bolted cold-formed steel angles", Journal of Construction Steel Research, Vol. 64, pp. 571 - 583, 2008. 5, <https://doi.org/10.1016/J.JCSR.2007.10.008>